Dynamic MRI Scan Plane Control for Passive Tracking of Instruments and Devices

S.P. DiMaio[1], E. Samset[1,2], G. Fischer[3], I. Iordachita[3], G. Fichtinger[3], F. Jolesz[1], and C.M. Tempany[1]

[1] Brigham and Women's Hospital, Harvard Medical School, Boston, MA, USA
[2] Oslo University, Norway
[3] Johns Hopkins University, Baltimore, MA, USA

Abstract. This paper describes a novel image-based method for tracking robotic mechanisms and interventional devices during Magnetic Resonance Image (MRI)-guided procedures. It takes advantage of the multi-planar imaging capabilities of MRI to optimally image a set of localizing fiducials for passive motion tracking in the image coordinate frame. The imaging system is servoed to adaptively position the scan plane based on automatic detection and localization of fiducial artifacts directly from the acquired image stream. This closed-loop control system has been implemented using an open-source software framework and currently operates with GE MRI scanners. Accuracy and performance were evaluated in experiments, the results of which are presented here.

1 Introduction

Magnetic Resonance Imaging (MRI) is finding increased application for guiding clinical interventions, particularly percutaneous needle- and catheter-based procedures, due to its high soft-tissue contrast and multi-parametric imaging capabilities. In particular, applications of targeted ablation, biopsy and brachytherapy have been demonstrated for the management of breast and prostate cancer [1]. A variety of positioning devices and stereotactic templates have been developed for image-guided needle placement and efforts are currently underway to develop robotic assistants and focused ultrasound delivery systems for precise in-bore targeted therapy. Accurate calibration, tracking and navigation of such devices—as well as needles and catheters—are essential. *This paper describes a novel image-based method for instrument tracking that makes use of the multi-planar imaging capabilities of MRI to dynamically servo the scan plane for optimal device localization and visualization*[1].

In prior work, device tracking in the MRI environment has been achieved using either active or passive markers. A variety of active tracking approaches have been presented in the past [2,3,4,5]. While typically fast and accurate, such methods can have drawbacks such as line-of-sight limitations, heating, sensitive

[1] This publication was made possible by NIH grants R01-CA111288 and U41-RR019703. Its contents are solely the responsibility of the authors and do not necessarily represent the official views of the NIH.

N. Ayache, S. Ourselin, A. Maeder (Eds.): MICCAI 2007, Part II, LNCS 4792, pp. 50–58, 2007.

tuning, complex calibration and expense. A well known active approach tracks small receiver coils using the MRI scanner's readout gradients aligned along the coordinate axes [3,4]. Krieger et al. discuss their use of such active tracking coils for navigating a robotic device in [6].

Passive tracking approaches, in which devices (e.g., needles, catheters, and robotic guidance mechanisms) are detected and tracked directly from the images, provide an alternative solution [7,8,6]. The advantages of an image-based passive tracking approach are that needles and devices do not require expensive instrumentation, and that both the interventional device and the patient's anatomy are observed together in the same image space, thus eliminating a critical calibration step. There is, however, a compromise between imaging speed and quality that can degrade localization accuracy and reliability. In addition, MRI systems have been designed primarily for diagnostic imaging and are typically not equipped for closed-loop adaptive imaging that is often required for interventional navigation and guidance. Contemporary MRI hardware and software designs are optimised for sequential batch imaging prescriptions, which create awkward interventional workflows. As a result, most clinical MRI-guided procedures follow an iterative imaging approach in which the patient is moved in and out of the scanner for imaging and intervention (e.g., see [6] and references).

In this work we demonstrate a general-purpose image-based approach for localizing devices in the bore of the magnet in order to enable simultaneous imaging and navigation for true image-guided intervention. This technology has been implemented using an open-source software framework and is currently available for use in GE MRI scanners. It is currently being used to develop a system for robot-assisted navigation of MRI-guided prostate biopsy and brachytherapy [9], as described in greater detail in our companion paper [10].

2 Methods

The concept of closed-loop scan-plane control for device localization is demonstrated here using a fiducial frame constructed from acrylic plastic, with seven embedded glass cylinders filled with MR-visible fluid (Beekley, Bristol, CT). Each of the seven cylinders forms a 3mm diameter, 60mm long MR-visible line fiducial, with the entire Z-frame arranged as shown in Figure 1.

The position and orientation of the Z-frame can be computed from a single intersecting 2D image—based on the coordinates of the seven fiducial points observed in the image—as described in [11], where a similar fiducial frame was used in CT. The Z-frame was placed in an MRI scanner (GE Signa EXCITE 3T), on a rotating platform with marked angle gradations, initially aligned at the isocentre. A continuous real-time pulse sequence was used to image a cross-section of the frame (Fast Gradient Recalled Echo, TR=14.1ms, TE=5.7ms, flip angle=45°, bandwidth=31.25kHz, matrix=256×256, NEX=1, FOV=16cm, slice thickness=2mm). The intersection points of the seven line fiducials—visible as seven bright disks (see Figure 1)—were automatically detected by a fast k-space template matching algorithm and used to compute the position and orientation

of the Z-frame relative to the scan plane. The frame was then manually rotated on the platform, while a closed-loop control system continuously and automatically adjusted the position and orientation of the imaging plane to align with the centre of the fiducial frame. This is illustrated in the series of images shown in Figure 2.

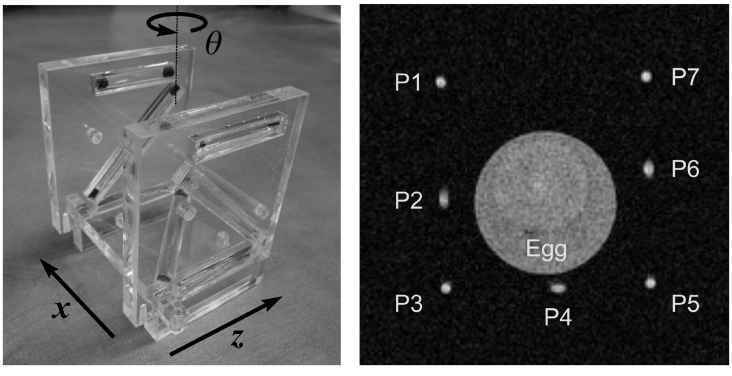

Fig. 1. (a) The Z-frame with 7 MR-visible line fiducials. (b) A sample MR image of a cross section of the Z-frame.

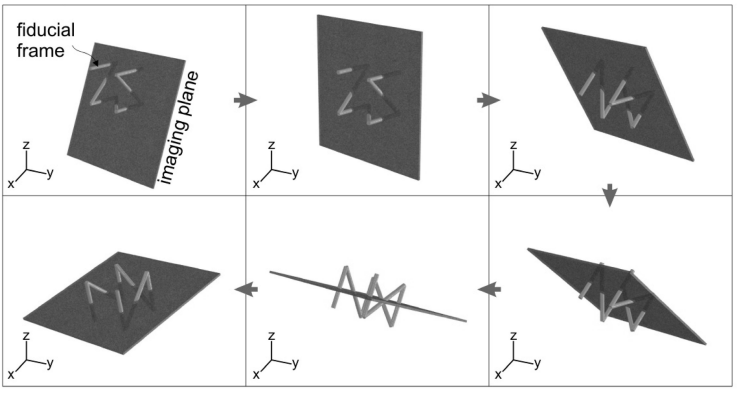

Fig. 2. The imaging plane is adapted to automatically follow the motion of the fiducial frame in the scanner

System Architecture

The software architecture for this system is shown in Figure 3. The MR scanner acquires 2D images continuously and transfers k-space data to a *Raw Data Server* that allows us to access image data in real-time. The raw data is passed through an *Image Reconstruction* algorithm (at present, the image reconstruction algorithm does not account for gradient warping) before being processed by

the *Image Controller*, which consists of algorithms for automatic fiducial detection, frame localization and scan plane control, as described below. The *Image Controller* passes images to a user interface for visualization and also closes the loop with the MRI scanner via the *RSP Server*, which provides the means to dynamically update pulse sequence parameters (RSPs), including those that determine scan plane position and orientation. Data interfaces between the tracking

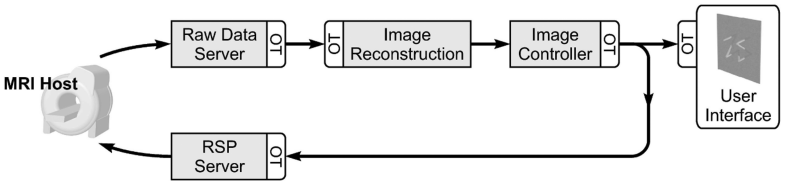

Fig. 3. System architecture

application and the imaging system were developed using an extension of the OpenTracker framework [12] (these interfaces are indicated by "OT" annotations in Figure 3). This framework provides mechanisms for dynamic event passing between distributed computing systems over the MRI host's TCP/IP network. The image visualization and graphical user interface was implemented using the Slicer Image Guided Navigator (SIGN), developed by Samset et al. [13]. Both OpenTracker and The SIGN are open-source software packages.

Fiducial Detection and Localization

The closed-loop fiducial detection and localization algorithm is detailed in the block diagram shown in Figure 4.

Fiducials are detected by fast template matching (similar to that used in [7]), where the template mask $m(u, v)$ is convolved with the latest MR image $i_i(u, v)$. In the spatial frequency domain (i.e., k-space) this corresponds to multiplication of $M(k_u, k_v)$ and $I_i(k_u, k_v)$, computed by Fast Fourier Transform of m and i_i respectively. Fiducial matches are detected as local maxima in $f(k_u, k_v)$, with subpixel interpolation of peak coordinates (quadratic interpolation). The resulting fiducial pattern is validated against known geometric contraints of the Z-frame and the seven fiducial point matches are ordered as shown in Figure 1. The ordered set of fiducial point coordinates P' are then used to compute the 6-DOF pose of the Z-frame with respect to the plane of image i_i (for details of a closed-form solution, see [11, 14]). Finally, the computed frame position/orientation is used to compute the new scan plane (i.e., for image i_{i+1}) that passes through the centre of the Z-frame.

Tracking accuracy and performance were measured in two sets of experiments: (a) tracking of freehand motion and (b) a calibrated accuracy study.

Tracking of Freehand Motion

The Z-frame was placed off-center on the rotating platform inside the scanner bore. With the closed loop tracking algorithm running, as shown in Figures 3

and 4, the platform was manually rotated by approximately 10° increments from $0 - 70°$.

Accuracy Study

In order to measure tracking accuracy, the Z-frame was fixed stationery within the scanner while varying the imaging position and orientation over three axes, namely x, z, and θ, as defined in Figure 1. For x- and z-axis displacements the images were aligned axially (i.e., with the x-axis in-plane and the z-axis normal to the imaging plane). In-plane motion (along the x-axis) was measured at approximately 1mm increments; out-of-plane motion (along the z-axis) was measured at approximately 2mm increments; rotational motion θ was measured at roughly 2° increments. For each axis, ten distinct positions/orientations were imaged, each ten times for a total of one hundred samples per axis. For each sample, the known image position/orientation was compared against the estimated Z-frame position/orientation, computed with respect to the image. The position of the Z-frame was initialized from an axial baseline image, such that all subsequent displacements were expressed with respect to this baseline.

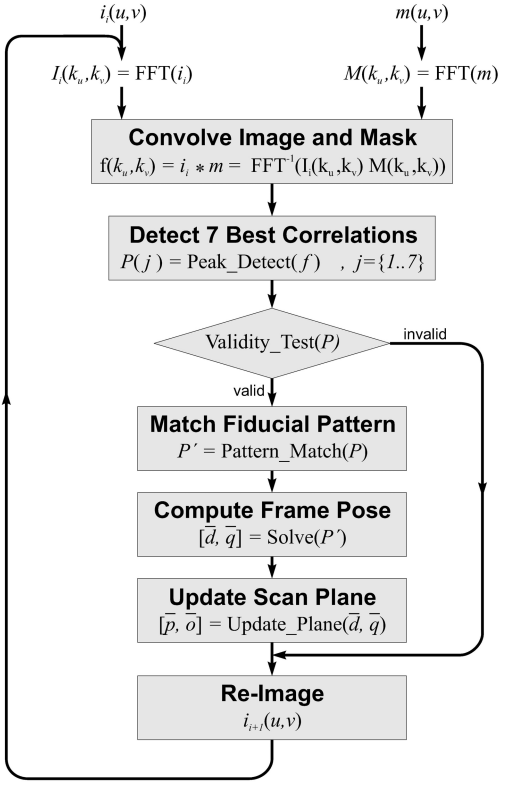

Fig. 4. Algorithm for detecting and localizing the fiducial frame

3 Results

The closed-loop scan plane control system was able to follow continuous motion of the Z-frame, provided that it did not move out of the imaging plane or cause significant motion artifact during each 2-3s image acquisition period.

Figure 5 shows the rotational motion component (θ) measured during the freehand motion experiment. Tracking performance was noticeably degraded for angles greater than $40 - 50°$.

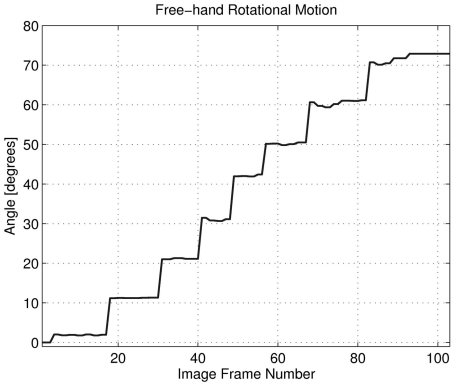

Fig. 5. Dynamically controlled image plane orientation θ during freehand manipulation of the Z-frame. Closed-loop imaging does not currently include GradWarp correction.

Results of the accuracy study are shown in Figure 6. The detection of in-plane motion (along the x-axis) and rotational motion (θ) are shown in plots (a) and (b). In each case the scan plane postion/orientation and estimated displacement/rotation are superimposed. Error statistics are summarized in Table 1.

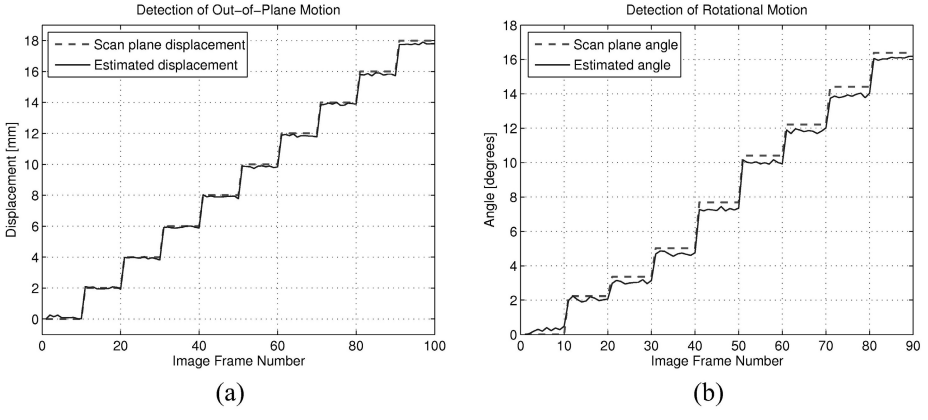

Fig. 6. Accuracy study results: (a) detection of out-of-plane motion along the z-axis, (b) detection of rotational motion about θ. GradWarp correction included, results summarized in Table 1.

Table 1. Z-frame Localization Accuracy

Axis	Average Error	Standard Deviation	RMS Error	Samples
In-plane (x)	0.017mm	0.026mm	0.031mm^2	$N = 100$
Out-of-plane (z)	0.089mm	0.11mm	0.14mm^2	$N = 100$
Rotation (θ)	0.28°	0.23°	$0.37^{\circ\,2}$	$N = 90$

4 Discussion and Conclusions

Experimental results demonstrate surprisingly good sub-millimeter and sub-degree accuracy when tracking the Z-frame from a single 2D image. While it is not quantified in this study, localization accuracy depends upon the pixel size, which in our experiments is $\frac{\text{field of view}}{\text{image dimension}} = 0.625mm$. Real-time tracking was noticeably degraded for large scan plane angles with respect to the axial plane, presumably due to the absence of gradient warp (GradWarp) correction. This limitation will be addressed in future work. The results of the accuracy study—listed in Table 1—were measured using a non-real-time pulse sequence in order to include GradWarp correction. This highlights one of the major challenges experienced in such research work, namely the absence of MRI pulse sequences and data flow mechanisms optimized for closed-loop interventional navigation. GE product pulse sequences were used without modification; however, custom interfaces were designed to interact with the raw data server and RSP modification mechanism, neither of which are supported GE products. The interfaces implemented in this work make use of open-source software architectures and are now publically available (`http://www.ncigt.org/sign/download`). At the time of publication, this interface is available only for GE MRI scanners; however, due to the modular architecture of its design, interface drivers for other imaging systems can be integrated without significantly affecting the overall control architecture. The *OpenTracker* interfaces shown in Figure 3 constitute a complete abstraction of hardware; therefore, this software framework can easily be adapted to MRI systems from other vendors. Plans are already underway for this extension.

A localization approach that does not rely upon additional instrumentation, and that is intrinsically registered to the imaging coordinate frame is highly desirable for navigating instruments in MRI-guided interventions. This work demonstrates that it is possible to use passive fiducial detection in 3T MRI images for dynamically locating and navigating targeted interventional devices with sufficient accuracy. The approach is primarily feasible for tracking relatively slow motion, as is the case with most clinical robotic assistants. In such applications [10], we are able to control motion in order to synchronize with image-based localization and tracking. However, the approach is not yet suitable for tracking rapid motions, such as may be found in free-hand applications. We are working to accelerate the image update rate—thereby reducing the effect of motion artifact—by means of parallel imaging techniques.

In future work, we will develop custom pulse sequences that are further optimized for real-time tracking of fiducials and needles, by taking advantage of parallel imaging methods. This will help to reduce the effect of motion artifact and to increase the field of view. In this work, we did not explore whether localization accuracy is consistent throughout the imaging field of view. This may be an issue when imaging fiducials relatively far from the iso-center of the magnet, and needs to be studied further.

The fiducial frame will be reduced in size and integrated with a robotic needle driver for targeted MRI-guided needle biopsy and brachytherapy applications

[10]. The minimum size of the fiducial frame is governed by image resolution, signal-to-noise requirements, the maximum tolerable motion between imaging frames, and the number of degrees of freedom to be measured. For the application described in [10] the current fiducial frame design is conservative and will be made more compact. In addition, we are extending the approach for the tracking and visualization of needle artifacts [8].

Finally, new standards and open-interfaces for scanner control and adaptive real-time imaging are required to move MRI beyond its standing as a largely diagnostic imaging modality, in order to enable promising new interventional applications.

References

1. D'Amico, A.V., Tempany, C.M., Cormack, R., Hata, N., Jinzaki, M., Tuncali, K., Weinstein, M., Richie, J.P.: Transperineal magnetic resonance image guided prostate biopsy. Journal of Urology 164(2), 385–387 (2000)
2. Silverman, S.G., Collick, B.D., Figueira, M.R., Khorasani, R., Adams, D.F., Newman, R.W., Topulos, G.P., Jolesz, F.A.: Interactive MR-guided biopsy in an open-configuration MR imaging system. Radiology 197(1), 175–181 (1995)
3. Dumoulin, C.L., Souza, S.P., Darrow, R.D.: Real-time position monitoring of invasive devices using magnetic resonance. Magnetic Resonance in Medicine 29, 411–415 (1993)
4. Derbyshire, J.A., Wright, G.A., Henkelman, R.M., Hinks, R.S.: Dynamic scan-plane tracking using MRI position monitoring. J. Mag. Res. Imag. 8(4), 924–932 (1998)
5. Hushek, S.G., Fetics, B., Moser, R.M., Hoerter, N.F., Russell, L.J., Roth, A., Polenur, D., Nevo, E.: Initial Clinical Experience with a Passive Electromagnetic 3D Locator System. In: $5^t h$ Interventional MRI Symp., Boston MA, pp. 73–74 (2004)
6. Krieger, A., Fichtinger, G., Metzger, G., Atalar, E., Whitcomb, L.L.: A hybrid method for 6-dof tracking of mri-compatible robotic interventional devices. In: Proceedings of the IEEE Int. Conf. on Rob. and Auto., Florida, IEEE Computer Society Press, Los Alamitos (2006)
7. de Oliveira, A., Rauschenberg, J., Beyersdorff, D., Bock, W.S.M.: Automatic detection of passive marker systems using phase-only cross correlation. In: The 6th Interventional MRI Symposium, Leipzig, Germany (2006)
8. DiMaio, S., Kacher, D., Ellis, R., Fichtinger, G., Hata, N., Zientara, G., Panych, L., Kikinis, R., Jolesz, F.: Needle artifact localization in 3t mr images. In: Studies in Health Technologies and Informatics (MMVR), vol. 119, pp. 120–125 (2005)
9. DiMaio, S., Fischer, G., Haker, S., Hata, N., Iordachita, I., Tempany, C., Kikinis, R., Fichtinger, G.: A system for mri-guided prostate interventions. In: Int. Conf. on Biomed. Rob. and Biomechatronics, Pisa, Italy, IEEE/RAS-EMBS (2006)
10. Fischer, G., et al.: Development of a robotic assistant for needle-based transperineal prostate interventions in mri. In: International Conference on Medical Image Computing and Computer-Assisted Intervention. LNCS, Springer, Heidelberg (2007)
11. Susil, R., Anderson, J., Taylor, R.: A single image registration method for ct-guided interventions. In: Taylor, C., Colchester, A. (eds.) MICCAI 1999. LNCS, vol. 1679, pp. 798–808. Springer, Heidelberg (1999)

12. Reitmayr, G., Schmalstieg, D.: Opentracker-an open software architecture for reconfigurable tracking based on xml. In: IEEE Virtual Reality Conference, IEEE Computer Society Press, Los Alamitos (2001)
13. Samset, E., Hans, A., von Spiczak, J., DiMaio, S., Ellis, R., Hata, N., Jolesz, F.: The SIGN: A dynamic and extensible software framework for Image-Guided Therapy. In: Workshop on Open Source and Data for MICCAI, Insight-Journal (2006), http://hdl.handle.net/1926/207
14. Lee, S., Fichtinger, G., Chirikjian, G.S.: Numerical algorithms for spatial registration of line fiducials from cross-sectional images. Medical Physics 29(8), 1881–1891 (2002)